Article

Not peer-reviewed version

Gut Microbiota and Metabolite Dynamics in a MASLD-Associated Liver Fibrosis In Vivo Model: An Integrative Multi-Omic Perspective

Alba González-Robles , Beatriz San-Miguel , Sara Román-Sagüillo , María Juárez-Fernández , José L Mauriz , Susana Martínez Flórez , Esther Nistal , María Victoria García-Mediavilla * , Sonia Sánchez-Campos

Posted Date: 5 February 2026

doi: 10.20944/preprints202602.0461.v1

Keywords: gut microbiota; *Akkermansia muciniphila*; melatonin; liver fibrosis; MASLD

Article

Gut Microbiota and Metabolite Dynamics in a MASLD-Associated Liver Fibrosis In Vivo Model: An Integrative Multi-Omic Perspective

Alba González-Robles, Beatriz San Miguel, Sara Román-Sagüillo, María Juárez-Fernández, José Luis Mauriz, Susana Martínez-Flórez, Esther Nistal, María Victoria García-Mediavilla *,† and Sonia Sánchez-Campos †

Instituto Universitario de Biomedicina (IBIOMED), Universidad de León, 24007 León, Spain

* Correspondence: mvgarm@unileon.es; Tel.: +34-987293258

† These authors contributed equally to this work.

Abstract

Metabolic dysfunction-associated steatotic liver disease (MASLD) is the most common cause of chronic liver disease worldwide. Fibrosis is the main prognostic factor and the last reversible stage before cirrhosis, yet therapeutic options remain limited. Given the strong contribution of gut dysbiosis to MASLD progression, strategies targeting the gut microbiota are of growing interest. This study aims to evaluate the effect of melatonin, a well-known antioxidant, anti-inflammatory and antifibrotic compound, and *Akkermansia muciniphila*, a next-generation probiotic, on a MASLD-associated liver fibrosis model. Eight-week-old C57BL/6J mice were fed with control or Western diet supplemented with fructose and intraperitoneal CCl_4 to induce liver fibrosis. After eight weeks, animals received either no intervention, melatonin, *A. muciniphila*, or both for four weeks. Serum biochemistry, liver histology and gut and liver gene expression were evaluated and multi-omic analyses were performed, including gut microbiota profiling and faecal metabolomics. Statistical analyses assessed intergroup differences and correlations across datasets. Both interventions partially restored gut microbiota composition and functionality and modulated hepatic and intestinal gene expression. Melatonin and *A. muciniphila* exerted protective effects against MASLD-associated fibrosis, which supports their potential as adjunctive therapeutic strategies to mitigate liver injury through modulation of the gut–liver axis.

Keywords: gut microbiota; *Akkermansia muciniphila*; melatonin; liver fibrosis; MASLD

1. Introduction

Metabolic dysfunction-associated steatotic liver disease (MASLD) is the leading cause of chronic liver disease worldwide and currently affects 30% of the adult population [1]. Its prevalence has risen substantially over the last three decades, with an expected exponential increase in accordance with the escalating rates of obesity and metabolic disorders [2]. MASLD encompasses a wide spectrum of liver injuries, including simple steatosis, steatohepatitis, fibrosis and cirrhosis [3]. Liver fibrosis is the result of chronic inflammation that triggers excessive accumulation of extracellular matrix leading to structural alteration and functional impairment [4]. Presence and grade of liver fibrosis are the most important prognosis determinants in MASLD. Moreover, liver fibrosis is the last reversible stage before cirrhosis, and hence, its clinical relevance [5,6].

Gut microbiota acts as a metabolically active organ [7] that plays a crucial role in maintaining host health as it performs a wide range of essential functions that contribute to human physiology [8]. Many extrinsic factors can affect gut microbiota, leading to an imbalance, known as dysbiosis, which involves compositional and functional changes [9]. MASLD is linked to dysbiosis, given the bidirectional crosstalk between gut and liver through the gut-liver axis [10]. Dietary patterns and

 doi:10.20944/preprints202602.0461.v1

metabolic disturbances characteristic of MASLD alter gut microbial communities and, at the same time, dysbiosis contributes to gut barrier disruption and increased intestinal permeability, enabling bacteria and their components to reach the liver, where they activate inflammatory pathways and stimulate innate immune responses that aggravate MASLD development. Gut dysbiosis also contributes to disease progression by increasing energy yield from diet, modulating bile acid metabolism and enhancing endogenous ethanol production [7,9,10].

Given the critical role of gut dysbiosis in MASLD progression, modulation of gut microbiota through various strategies, such as the administration of prebiotics, probiotics and synbiotics, constitutes a promising therapeutic approach [11]. In this context, and beyond its well-established immunomodulatory, anti-inflammatory, antioxidant and antifibrotic properties [12,13], melatonin acts as a prebiotic by reversing gut dysbiosis and enhancing intestinal barrier integrity [14]. These effects, combined with its proven ability to reduce body weight gain, improve hepatic steatosis, reduce inflammation and enhance insulin sensitivity, underscore melatonin as a potential candidate for MASLD management [15]. Likewise, *Akkermansia muciniphila*, a next-generation probiotic, has been introduced as a promising therapeutic option for MASLD, thanks to its capacity to improve insulin sensitivity and maintain gut homeostasis and gut barrier functionality, alleviating hepatic steatosis and inflammation [11,16].

This study aims to evaluate the combined effect of melatonin and *A. muciniphila* administration on metabolic parameters, the severity of the hepatic disease, the gut barrier integrity and the gut microbiota composition and functionality in an in vivo model of MASLD-associated liver fibrosis.

2. Materials and Methods

2.1. Experimental Design

All procedures were performed in accordance with the European Research Council guidelines for the care and use of laboratory animals and were approved by the Institutional Animal Care and Use Committee of the University of León (OEBA-ULE-004-2021), followed by authorization from the competent authority, the Junta de Castilla y León.

Animal model

Eight-week-old male C57BL/6J mice were divided into two groups based on their diet: Control (C) (18% of energy from fat; 114 Teklad Global #2018 Diet, Harlan Laboratories) (n = 40) and Western Diet (WD) (43% of energy from fat and 2% cholesterol; TD.160279; Envigo Teklad Diets, Madison, WI, USA) (n = 40). This second group received fructose-supplemented drinking water (150 mg ml^{-1}) and an intraperitoneal injection of CCl_4 (0.5 ml kg^{-1}) at weeks 1, 2, 4 and 6. C group received intraperitoneal injections of the vehicle of CCl_4 (corn oil) at the same intervals. After 8 weeks, both groups (C and WD) were split into four subgroups, based on diet solely (C [n = 8] and WD [n = 12] groups), melatonin administration (CM [n = 8] and WDM [n = 12] groups), *Akkermansia muciniphila* administration (CA [n = 8] and WDA [n = 12] groups) and combined melatonin and *A. muciniphila* administration (CMA [n = 8] and WDMA [n = 12] groups) (Figure 1). Mice were housed under controlled conditions of temperature, humidity and lighting, and had free access to water and food, which they consumed *ad libitum*. Body weight, food and water intake were monitored weekly. At the 12th week animals were euthanised by cardiac puncture under anaesthesia and blood, liver, ileum, adipose tissue and faecal and caecal contents were collected.

 doi:10.20944/preprints202602.0461.v1

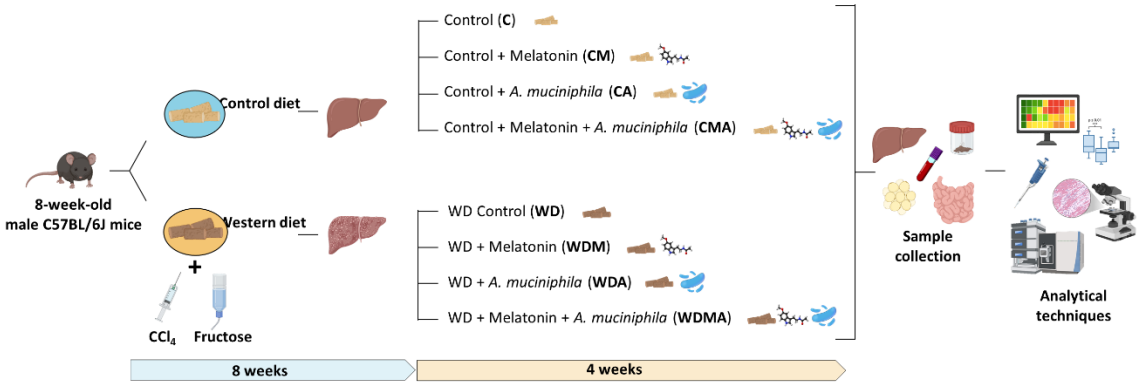

Figure 1. Experimental design. 8-week-old C57BL/6J mice were fed either a Control or Western Diet for 8 weeks. WD-fed mice received fructose-supplemented drinking water and intraperitoneal injections of CCl_4. Then, both groups were split into four subgroups, based on diet alone (C and WD groups), melatonin administration (CM and WDM groups), *Akkermansia muciniphila* administration (CA and WDA groups) and combined melatonin and *A. muciniphila* administration for 4 weeks.

Bacterial strain and growth conditions

Akkermansia muciniphila (CIP 107961^T) was cultured in brain heart infusion medium (OXOID Ltd., Basingstoke, Hampshire, England) at 37 °C for 48 h under anaerobic conditions, as previously described [17]. Cultures were centrifuged at 9000 rpm for 10 min, washed twice with sterile phosphate-buffered saline (PBS, pH 7.2), and resuspended in 200 µL of 10 % skim milk in PBS supplemented with 3 % cysteine to a final concentration of 2 × 10^8 CFU, for preservation. The suspension was stored at -80 °C and, prior to administration, was centrifuged again and resuspended in PBS, maintaining the same bacterial concentration. All procedures were carried out under strictly anaerobic conditions.

Dosage information

Melatonin was dissolved in absolute ethanol, and further dilutions were prepared in 0.9% NaCl solution until a final ethanol concentration of 2.5% was reached. Melatonin was administered intraperitoneally, in the evenings, at a dose of 20 mg kg^{-1} day^{-1}. Groups not supplemented with melatonin received daily injections of the vehicle (2.5% ethanol in 0.9% NaCl solution) alone.

Akkermansia muciniphila was administered five times per week by oral gavage at a dose of 2 × 10^8 CFU in 200 µL of PBS as the vehicle. Groups not supplemented with *A. muciniphila* received the vehicle alone.

2.2. Sample Collection

Blood samples were collected at the 8th week and at the end of the experimental period, and serum was immediately isolated for subsequent biochemical analysis. Liver and adipose tissue were harvested and weighed. Faecal and caecal contents were collected for gut microbiota compositional and metabolomic analyses. The left lobe of the liver and the ileum were immersed in RNA*later*™ stabilization solution (AM7021; Invitrogen, Thermo Fisher Scientific Inc.; Waltham, MA, USA) for 24 h and then stored at -80 °C for subsequent gene expression analyses. The right lobe of the liver was fixed in 10% formalin for histological evaluation.

2.3. Biochemical Analysis

Alanine aminotransferase (ALT), aspartate aminotransferase (AST) and gamma-glutamyl transferase (GGT) activities, as well as glucose, triglycerides and cholesterol levels were determined in serum samples by the Instrumental Techniques Laboratory of the University of León using standard procedures.

 doi:10.20944/preprints202602.0461.v1

2.4. Histopathology

Paraffin-embedded liver samples were sectioned and stained with haematoxylin and eosin (H&E). Histological assessments were performed by two expert examiners blinded to the experimental design. The extent of hepatic lesions was evaluated according to the NAFLD activity score (NAS) to provide a numerical score based on three histological features: steatosis (0–3), lobular inflammation (0–3) and hepatocellular ballooning (0–2) [18]. Liver fibrosis was assessed using the Masson's trichrome staining and a semiquantitative scoring system provided by a histopathology service from the University of León, ranging from 0 to 10, where 0 indicates absence of fibrosis and 10 corresponds to extreme fibrosis

2.5. Gene Expression Analysis

RNA extraction

For total RNA isolation, approximately 50 mg of each sample were homogenised in 1 ml of TRIzol™ reagent (15596026; Invitrogen, Thermo Fisher Scientific Inc., Waltham, MA, USA), following the manufacturer's protocol, which is based on phase separation with chloroform, RNA precipitation with isopropanol and subsequent washing and resuspension. The concentration of total RNA was measured with a NanoDrop 1000 spectrophotometer (Thermo Fisher Scientific Inc.; Waltham, MA, USA).

Quantitative Real-Time PCR (RT-qPCR)

For the reverse transcription reaction, first-strand cDNA was synthesised using the High-Capacity cDNA Reverse Transcription Kit (4368814; Thermo Fisher Scientific Inc., Waltham, MA, USA). Relative gene expression assays were carried out using the Applied Biosystems QuantStudio 5 Real-Time PCR System (Thermo Fisher Scientific Inc., Waltham, MA, USA) and commercially TaqMan® Gene Expression Assays (Applied Biosystems, Thermo Fisher Scientific Inc., Waltham, MA, USA) (**Table S1**). Glyceraldehyde-3-phosphate dehydrogenase (*Gapdh*) was used as internal control and $2^{-\Delta\Delta}$Ct method was applied to determine relative changes in gene expression levels.

2.6. Gut Microbiota Compositional Analysis

Faecal DNA extraction

Genomic DNA from faecal samples was extracted using the QIAamp Fast DNA Stool Mini Kit (51604; Qiagen, Hilden, Germany) according to the manufacturer's instructions, with some modifications, as previously described [19]. Briefly, an initial bead-beating step, using PowerBead Pro Tubes (Qiagen, Hilden, Germany) was included, and the lysis temperature was increased to 95 °C to aid in the recovery of DNA from bacteria that are difficult to lyse. DNA concentration was determined using a NanoDrop 1000 spectrophotometer (Thermo Fisher Scientific Inc., Waltham, MA, USA), and DNA samples were stored at −20 °C until further analysis.

Amplification, sequencing of 16S rRNA and bioinformatic analysis

Amplification of the 16S rRNA V3-V4 hypervariable region was performed by PCR, as previously described [20]. PCR assays were carried out in triplicate, and their products were pooled and purified using the Wizard® Genomic DNA Purification Kit (Promega, Madison, WI, USA).

Gut microbiota compositional analysis was carried out using the Illumina MiSeq platform, according to manufacturer's instructions, using the MiSeq Reagent Kit v3 and 300 bp paired-end reads. The Illumina bcl2fastq© program was used to demultiplex the sequencing data, and FastQC software (version 0.11.9) was used for post-sequencing quality control [21].

Analysis of the generated raw sequence data was performed using the Quantitative Insights into Microbial Ecology (QIIME 2) software (version 2022.2) [22] and the DADA2 plugin [23], including joining of forward and reverse reads, chimera removal, data filtering, and taxonomic annotation. Reads were organized in operational taxonomic units (OTUs). A fitted classifier trained on the SILVA database (release 138 QIIME) was used for the taxonomic assignment, with a clustering threshold of 99% similarity. Only OTUs containing at least 10 sequence reads were considered as significant.

 doi:10.20944/preprints202602.0461.v1

2.7. Faecal Metabolomic Analysis

Faecal metabolome was determined by liquid chromatography–mass spectrometry (LC-MS) at MS-Omics (Copenhagen, Denmark). Approximately 50-100 mg of faecal content were used for metabolite extraction. For each sample, 2 µl of eluent solution per mg of faeces was added, followed by vortex mixing and centrifugation. The resulting supernatants were transferred to centrifugation filter tubes, and the filtrate was diluted 10-fold in eluent solution prior to LC-MS analysis. For quality control, a pooled sample was prepared by combining small aliquots from each individual sample.

The LC-MS method was performed using a UPLC system (Vanquish; Thermo Fisher Scientific Inc., Waltham, MA, USA) coupled with a high-resolution quadrupole-orbitrap mass spectrometer (Q Exactive™ HF Hybrid Quadrupole-Orbitrap; Thermo Fisher Scientific Inc., Waltham, MA, USA). An electrospray ionisation interface was used as the ion source. Analysis was conducted in negative and positive ionisation modes. Our quality control sample was analysed in MS/MS mode for compound identification. Data were processed using Compound Discoverer 3.2 (ThermoFisher Scientific Inc., Waltham, MA, USA).

2.8. Statistical Analysis

Data are expressed as the mean ± standard deviation (SD). Significant differences between two groups (8th week) were evaluated by Student's t-test, while comparisons among multiple experimental groups (12th week) were performed using one-way analysis of variance (ANOVA), followed by pairwise Student's t-tests and Fisher's LSD post-hoc test when applicable. Statistical differences in gut microbiota composition and metabolomic data were assessed by a non-parametric Kruskal–Wallis test, followed by pairwise Mann–Whitney U tests when $p < 0.05$; Dunn's test was applied for correction for multiple testing. Permutational multivariate analysis of variance (PERMANOVA) was used to assess the contribution of different factors to bacterial community distribution. Associations among biochemical parameters, gene expression, gut microbiota composition and metabolomic data were evaluated using Spearman's correlation, with false discovery rate (FDR) correction for multiple testing. Analyses were conducted using R software (R-project, Vienna, Austria) and GraphPad Prism 8 (San Diego, CA, USA).

3. Results

3.1. Western Diet Induces Metabolic and Histological Alterations and Hepatic and Intestinal Gene Expression Deregulation

After 8 weeks, the group that received WD feeding developed multiple alterations consistent with MASLD. Biochemical analyses revealed significant increases in ALT (+54.6%) and AST (+42.4%) levels in comparison with the Control diet-fed group (Table S2), indicating hepatocellular damage. Fasting glucose and total cholesterol concentrations were also markedly elevated (+20.5% and +133.5%, respectively) (Table S2), reflecting the onset of metabolic dysfunction and a possible early impairment of insulin sensitivity.

At the 12th week, at the end of the experimental period, the WD group, which did not receive any treatment, showed significantly higher body, liver, and white adipose tissue weights (+14.2%, +72.7% and +146.7%, respectively) and an increased hepatosomatic index (Figure 2A). These changes reflect increased adiposity and marked liver enlargement associated with lipid accumulation, with white adipose tissue expansion being evident both in absolute terms and relative to total body weight. Histological examination revealed increased steatosis, hepatocellular ballooning and total NAS score with respect to the control group (Figure 2B and Figure S1), along with the presence of liver fibrosis (Figure 2C and Figure S2). At the molecular level (Figure 2D), WD-fed mice exhibited upregulation of hepatic pro-inflammatory (*Tnf, Tlr2, Tlr4, Nlrp3*) and profibrogenic (*Timp1, Acta2*) genes, consistent with low-grade inflammation and early fibrogenic remodelling. Moreover, intestinal barrier integrity was compromised, as shown by the significant downregulation of genes encoding key tight junction

 doi:10.20944/preprints202602.0461.v1

proteins (*Cldn1, Tjp1*) and mucosal barrier formation (*Muc2*) (Figure 2E), indicative of impaired epithelial integrity and reduced mucosal protection.

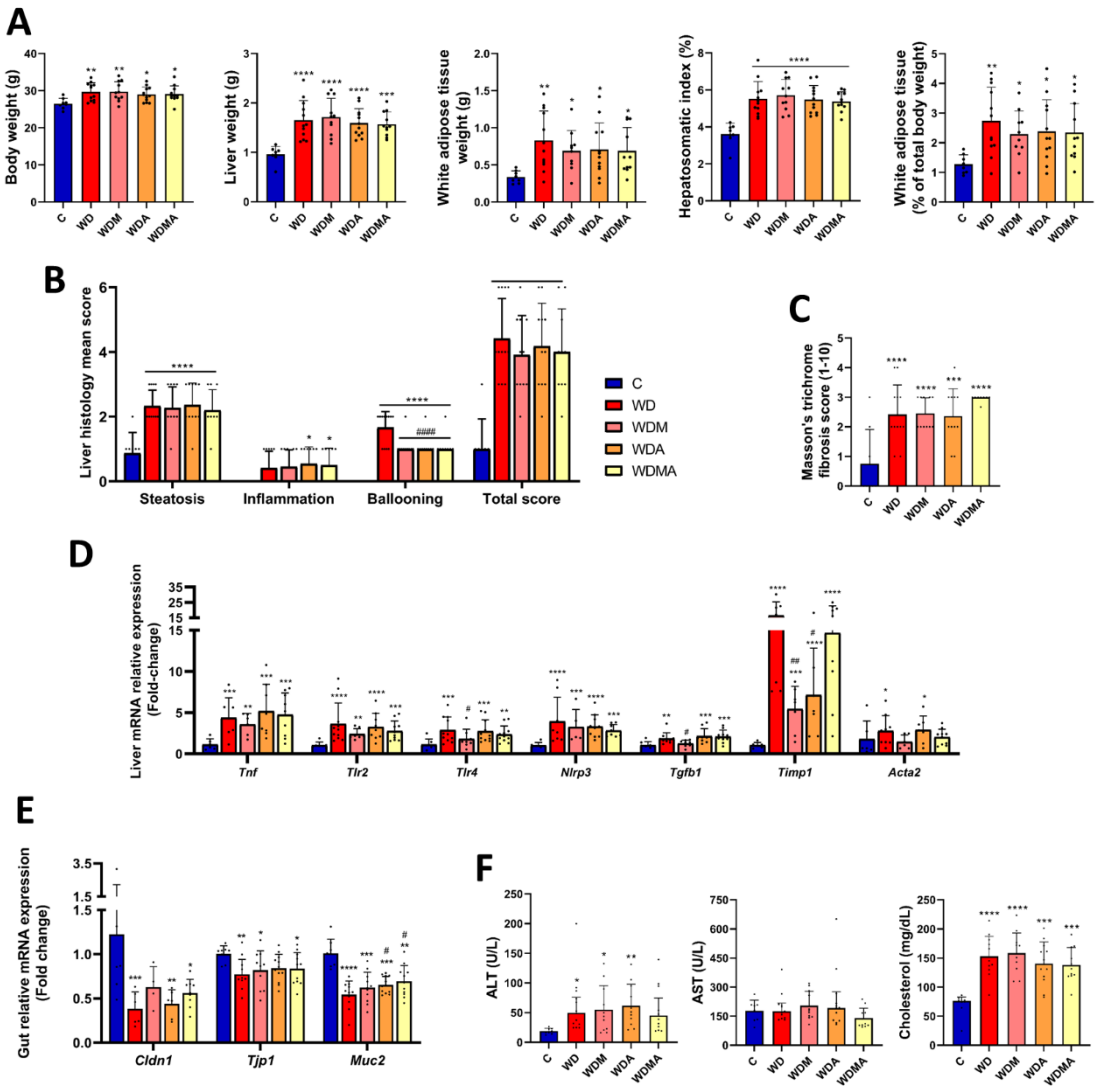

Figure 2. Effect of Western Diet, melatonin and *A. muciniphila* administration on MASLD-associated features development. **A**) Body, liver and white adipose tissue weights and hepatosomatic index (liver weight / body weight × 100). **B**) NAFLD activity score (NAS) calculated from individual scores for steatosis, lobular inflammation and hepatocellular ballooning. **C**) Fibrosis evaluation on Masson's trichrome-stained sections using a semiquantitative scoring system ranging from 1 to 10, as provided by the histopathology service. **D**) Relative mRNA expression in liver tissue of genes involved in inflammation (*Tnf, Tlr2, Tlr4, Nlrp3, Tgfb1*) and fibrosis (*Timp1, Acta2*). **E**) Relative mRNA expression in gut tissue of genes involved in intestinal barrier function (*Cldn1, Tjp1, Muc2*). **F**) ALT and AST levels and cholesterol concentration in serum. At least n = 5 were used in each experimental group. * $p < 0.05$ vs. C; ** $p < 0.01$ vs. C; *** $p < 0.001$ vs. C; ****$p < 0.0001$ vs. C; $^{\#}$ $p < 0.05$ vs. WD; $^{\#\#}$ $p < 0.01$ vs. WD; $^{\#\#\#\#}$ $p < 0.0001$ vs. WD.

3.2. Melatonin and A. muciniphila Exert Limited Biochemical and Histological Effects but Induce Hepatic and Intestinal Gene Expression Changes

Melatonin and *A. muciniphila* administration to the Control Diet-fed mice did not modify any of the biochemical, morphometric or histological analysed parameters. As no differences were observed

 doi:10.20944/preprints202602.0461.v1

among control groups (Figure S3), only the untreated control group (C) was used for subsequent analyses. In WD-fed mice, interventions showed partial improvements in different outcomes. Both the WDA and WDMA groups displayed a trend towards lower serum cholesterol concentrations, while the WDMA group showed a modest, non-significant reduction in ALT and AST levels (Figure 2F), suggesting a possible initial improvement in liver damage. Liver weight tended to decrease in response to *A. muciniphila* administration, whereas white adipose tissue weight, both in absolute terms and expressed as a percentage of the total body weight, was slightly but non-significantly reduced across all intervention groups (Figure 2A). Histologically, hepatocellular ballooning was significantly reduced in the WDM, WDA and WDMA groups, although the total NAS score remained unchanged (Figure 2C).

At the molecular level, melatonin treatment significantly decreased hepatic expression of *Tlr4*, *Tgfb1* and *Timp1*, and showed a trend towards reduced expression of *Tnf*, *Tlr2*, *Nlrp3* and *Acta2* (Figure 2E). At the intestinal level, melatonin showed a trend towards increased *Cldn1* expression, suggesting a partial restoration of tight junction integrity (Figure 2F). *A. muciniphila* administration significantly reduced hepatic *Timp1* expression (Figure 2E), potentially attenuating profibrogenic activity, and significantly increased intestinal *Muc2* expression (Figure 2F), supporting mucosal barrier function. Finally, the combined treatment tended to decrease hepatic *Tlr2*, *Tlr4* and *Nlrp3* expression (Figure 2E), indicating a tendency to reduced hepatic inflammatory and profibrogenic signalling, and was associated with a significant upregulation of *Muc2*, together with a trend towards increased intestinal *Cldn1* expression (Figure 2F), which may collectively contribute to improve intestinal barrier integrity.

Overall, these findings indicate that melatonin and *A. muciniphila*, alone or in combination, partially modulate hepatic and intestinal molecular pathways and histological features, reflecting a modest improvement in liver function and gut barrier-related parameters in WD-fed mice.

3.3. Melatonin and A. muciniphila Modulate Gut Microbiota Diversity and Composition After WD-induced Dysbiosis

To assess global changes in gut microbial community structure, α and β-diversity analyses were performed. For α-diversity (Figure S4), the Simpson index showed a significant overall difference across groups (Kruskal–Wallis $p = 0.043$), although no significant pairwise comparisons were detected. In contrast, the Shannon index did not show significant overall differences (Kruskal–Wallis $p = 0.074$). β-diversity analysis (Figure 3A) based on Bray–Curtis dissimilarity and Principal Coordinates Analysis (PCoA) revealed a clear group-dependent clustering, primarily driven by the dietary intervention, as confirmed by PERMANOVA ($p = 0.001$), with the group factor explaining 66.67% of the total variance ($R^2 = 0.6667$).

The fibrosis-inducing protocol produced marked alterations in gut microbiota composition at multiple taxonomic levels. At the phylum level, WD-fed mice showed a significant increase in the relative abundance of Pseudomonadota, accompanied by a significant reduction in Bacteroidota (Figure 3B). At the class level, Desulfovibrionia was significantly enriched, whereas Actinobacteria and Bacteroidia were significantly reduced. (Figure 3C).

At the genus level, the WD group significantly increased the relative abundance of *Alistipes*, *Alloprevotella*, *Blautia*, *Faecalibaculum*, *Intestinimonas*, *Lachnoclostridium*, *Lactococcus* and *Tuzzerella*. Conversely, *Dermacoccus*, *Lactobacillus* and *Muribaculum* were significantly reduced (Figure 3D).

Both melatonin and *A. muciniphila* showed modulatory effects at genus level (Figure 3D). *Alistipes* abundance decreased in WDM compared to the WD group, approaching control values, and *Blautia* was reduced in WDA. However, intervention effects were most evident in the WDMA group, where the class Actinobacteria was significantly increased, reaching values comparable to controls (Figure 3C). At the genus level, *Dermacoccus* significantly increased in WDA and WDMA, accompanied by a similar trend in *Eisenbergiella*. *Muribaculum* showed a non-significant increase in WDMA, while *Odoribacter* was significantly reduced in this group compared to WD (Figure 3D).

 doi:10.20944/preprints202602.0461.v1

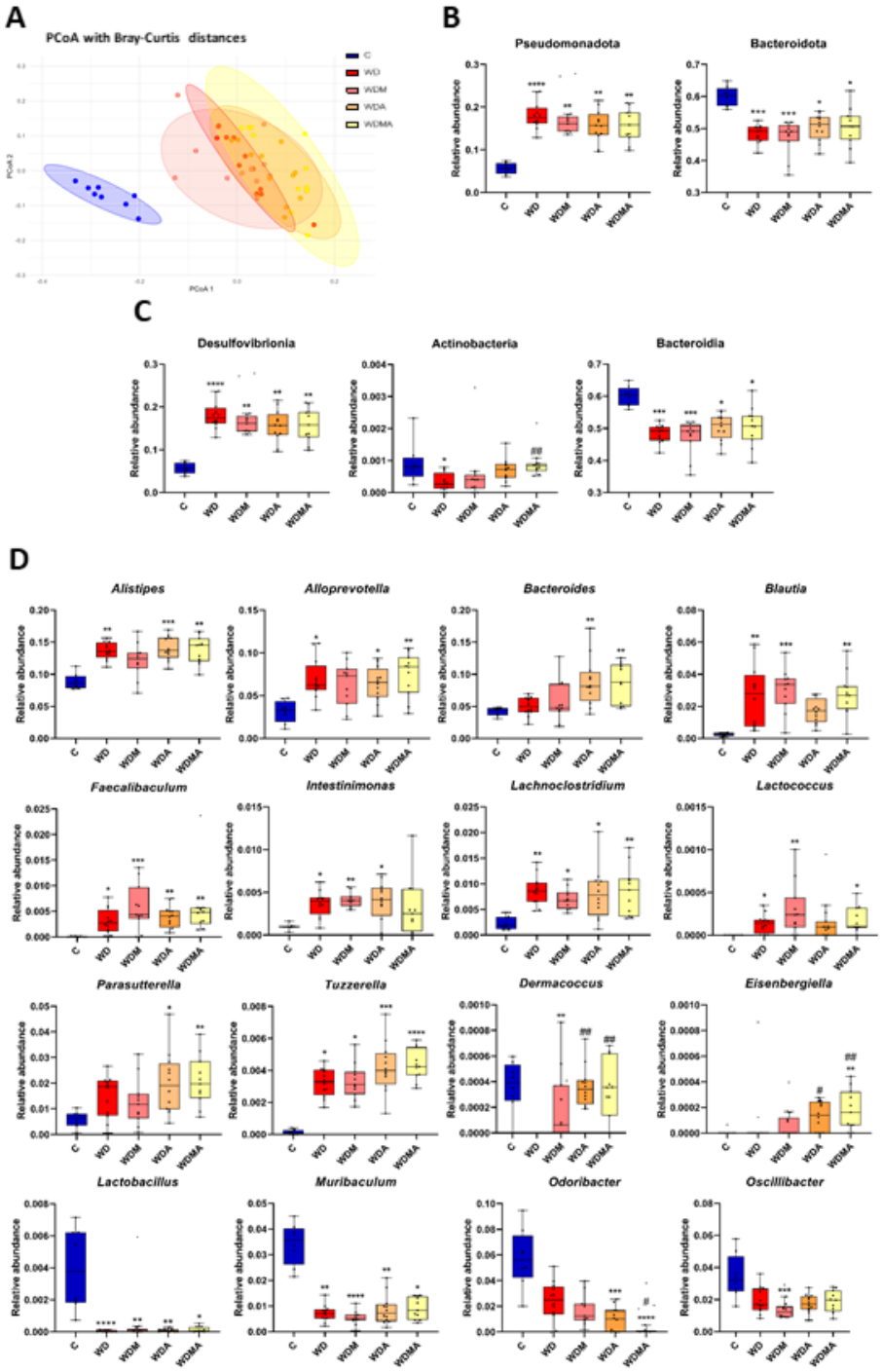

Figure 3. Effect of Western Diet, melatonin and *A. muciniphila* administration on gut microbiota diversity and composition. **A)** Principal coordinates analysis (PCoA) plot based on Bray–Curtis dissimilarity index at the genus level representing β-diversity. **B)** Relative abundance in the different experimental groups at phylum level, **C)** class level and **D)** genus level. At least n = 7 were used in each experimental group. * $p < 0.05$ vs. C; ** $p < 0.01$ vs. C; *** $p < 0.001$ vs. C; ****$p < 0.0001$ vs. C; $^{\#}$ $p < 0.05$ vs. WD; $^{\#\#}$ $p < 0.01$ vs. WD.

Together, these results indicate that Western diet feeding is the main determinant of gut microbial community structure in this model. While α-diversity analyses showed only subtle overall differences, taxonomic-level analyses reveal that the interventions already induced genus-specific shifts, particularly under the combined treatment, suggesting that the gut microbiota composition and structure was modulated, partially counteracting diet-related alterations.

 doi:10.20944/preprints202602.0461.v1

3.4. Melatonin and A. muciniphila Partially Restore WD-impaired Gut Microbiota Functionality

The fibrogenic intervention not only altered microbiota composition but also markedly disrupted its functional profile, as reflected by shifts in faecal metabolite concentrations. WD feeding significantly increased several metabolites (choline, hydroferulic acid, muricholic acid, N-formylmethionine, phosphocholine and tromethamine) while reducing numerous compounds linked to microbial metabolism and host-microbiota interactions (acetylmuramic acid, ascorbic acid, dihydroxyphenylalanine, ferulic acid, glucuronic acid, indole-3-acetic acid, indole-3-glyoxylic acid, lactic acid and N-acetyl-tyrosine) (Figure 4). These changes indicate possible functional microbial alterations accompanying the compositional shifts.

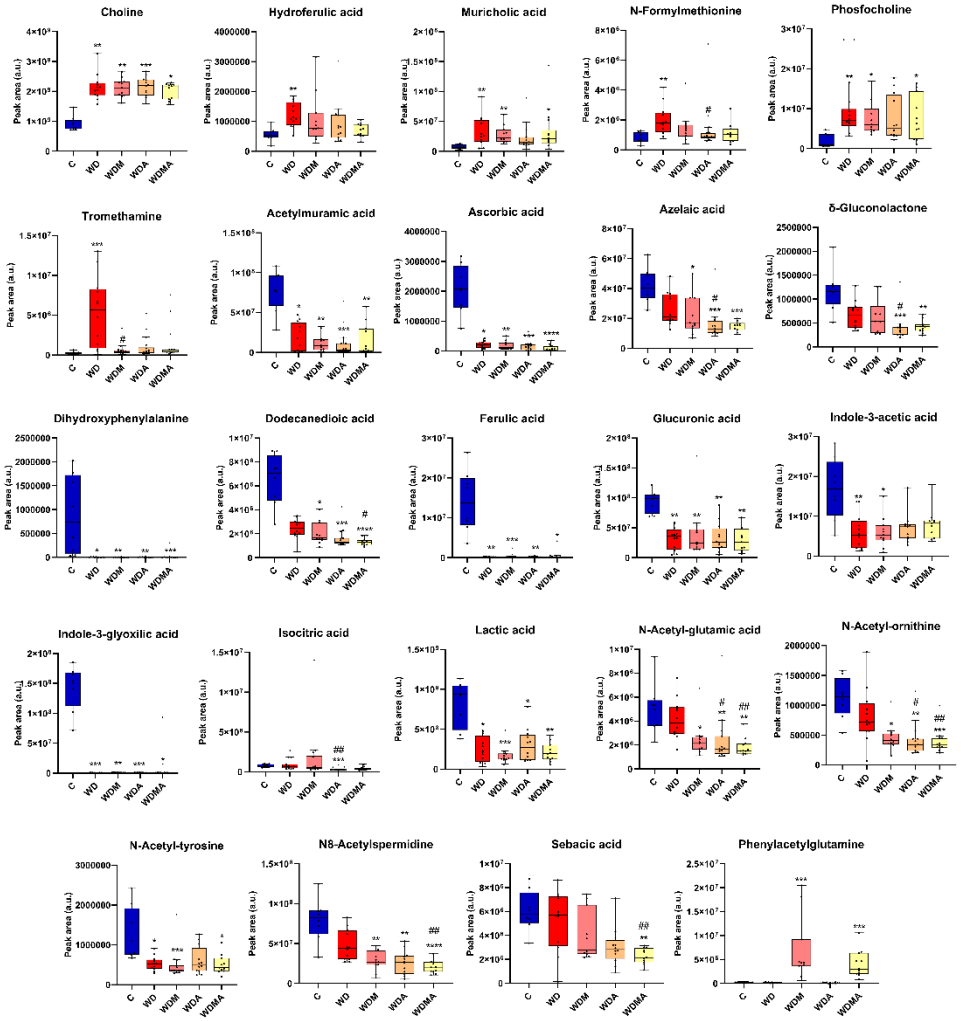

Figure 4. Effect of Western Diet, melatonin and *A. muciniphila* on the faecal metabolome. At least n = 8 were used in each experimental group. * $p < 0.05$ vs. C; ** $p < 0.01$ vs. C; *** $p < 0.001$ vs. C; ****$p < 0.0001$ vs. C; $^{\#}$ $p < 0.05$ vs. WD; $^{\#\#}$ $p < 0.01$ vs. WD; $^{\#\#\#}$ $p < 0.001$ vs. WD.

Administration of *A. muciniphila* and/or melatonin partially reversed WD-induced metabolomic disturbances, generally lowering metabolites elevated in WD mice towards control levels, with significant effects for N-formylmethionine, following *A. muciniphila* administration, and tromethamine, in response to melatonin. Interestingly, certain metabolites (azelaic acid, δ-gluconolactone, dodecanedioic acid, isocitric acid, N-acetyl-glutamic acid, N-acetyl-ornithine, N8-acetylspermidine and sebacic acid) decreased further relative to WD, diverging from the control

 doi:10.20944/preprints202602.0461.v1

profile. In contrast, phenylacetylglutamine increased significantly in the WDM and WDMA groups (Figure 4).

3.5. Correlation Analyses Reveal Interactions Between Host Biochemical and Molecular Markers, Gut Microbiota Composition and Faecal Metabolomic Profiles

Correlation analyses revealed consistent associations between gut microbial taxa, faecal metabolites and host biochemical parameters and hepatic and intestinal gene expression (Figure 5 and Figure S5). Among the genera altered by WD, *Alistipes*, *Blautia*, *Intestinimonas* and *Lachnoclostridium* showed positive correlations with serum cholesterol (Figure 5A), supporting their possible association with WD-induced dyslipidaemia. *Alistipes* and *Blautia*, additionally, correlated positively with hepatic expression of pro-inflammatory and profibrogenic genes (Figure S5B), and *Blautia* also correlated with ALT levels (Figure 5A), possibly linking these taxa to liver injury and fibrogenic responses. *Intestinimonas* was also associated with fasting glucose (Figure 5A), suggesting a contribution to metabolic alterations. In contrast, *Muribaculum* abundance correlated negatively with glucose and cholesterol concentrations (Figure 5A) and positively with the expression of intestinal barrier integrity-related genes (Figure S5D), highlighting a potential protective role. Similarly, *Lactobacillus* was inversely associated with hepatic inflammatory and fibrogenic markers (Figure S5B), suggesting a role in ameliorating liver injury.

Several metabolites that changed significantly in response to WD and melatonin and/or *A. muciniphila* were also linked to host biochemical and molecular parameters. N-formylmethionine and hydroferulic acid correlated positively with serum cholesterol (Figure S5A), and N-formylmethionine also with hepatic *Timp1* expression (Figure S5C). Tromethamine was likewise associated with *Timp1*, *Tlr4* and *Tnf* (Figure S5C), pointing to potential involvement in pro-inflammatory signalling. Conversely, dicarboxylic acids, including sebacic and dodecanedioic acids, showed negative correlations with hepatic inflammatory and fibrogenic markers (Figure S5C). A similar pattern was observed for δ-gluconolactone, N-acetyl-ornithine, N-acetyl-glutamic acid, N8-acetylspermidine and ascorbic acid, whose depletion was consistently linked to enhanced liver injury (Figure S5C).

Genus–metabolite correlations (Figure 5B) revealed consistent associations between bacterial taxa and specific metabolites. *Blautia*, *Intestinimonas* and *Lachnoclostridium* correlated positively with N-formylmethionine, hydroferulic acid and tromethamine, whereas *Muribaculum* displayed opposite associations with these metabolites, in line with its suggested protective role. In addition, several taxa were connected to dicarboxylic acids: *Odoribacter* correlated positively with dodecanedioic, azelaic and sebacic acids, and also showed positive associations with other metabolites such as δ-gluconolactone, N-acetyl-glutamic acid, N-acetyl-ornithine, ascorbic acid and isocitric acid. Conversely, *Bacteroides*, *Eisenbergiella*, *Faecalibaculum*, *Lactococcus*, *Parasutterella* and *Tuzzerella* were consistently negatively associated with dicarboxylic acids. Altogether, these associations illustrate coordinated networks linking microbial shifts, metabolite profiles and host responses in WD-induced metabolic associated liver disease, partially reshaped by melatonin and *A. muciniphila* treatment.

 doi:10.20944/preprints202602.0461.v1

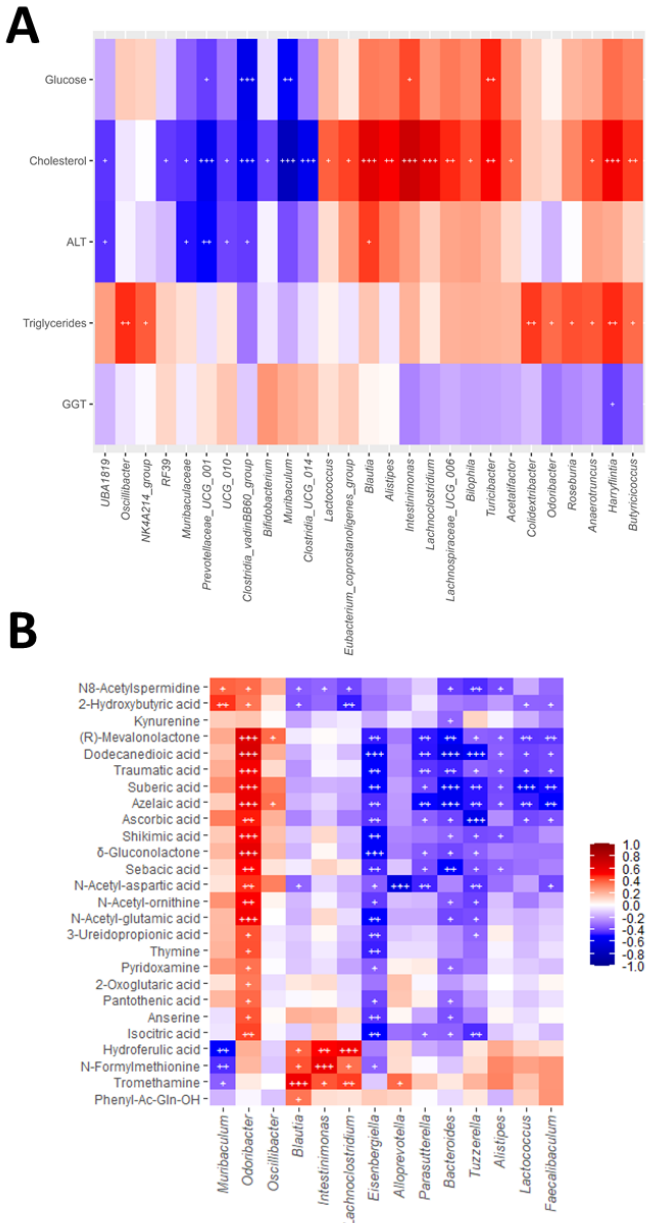

Figure 5. Correlation analysis. Heatmaps showing Spearman correlations between **A**) serum biochemical parameters and bacterial genera and **B**) faecal concentrations of metabolites and bacterial genera. Each square represents the Spearman's correlation coefficient ($q < 0.05$). Red and blue cells represent positive and negative correlations, respectively. White crosses designate the level of significance: $^{+}$ $q < 0.05$; $^{++}$ $q < 0.01$; $^{+++}$ $q < 0.001$.

4. Discussion

MASLD is characterised by hepatic lipid accumulation driven by hypercaloric diets rich in sugars and saturated fats, typically referred to as "Western Diet" [24,25]. Patients frequently display gut dysbiosis and impaired intestinal barrier integrity, underscoring the role of the gut–liver axis in disease development [10]. Lifestyle interventions remain the cornerstone of MASLD management; however, long-term adherence is limited [26]. Given the key role of gut dysbiosis in disease progression, modulation of the gut microbiota using prebiotics and probiotics has emerged as a promising therapeutic approach [9,10].

Melatonin, a well-known antioxidant and anti-inflammatory molecule [27], has demonstrated prebiotic properties, counteracting diet-induced dysbiosis and metabolic alterations [28–30]. Likewise, *Akkermansia muciniphila*, considered a next-generation probiotic, has shown protective

 doi:10.20944/preprints202602.0461.v1

effects against obesity, insulin resistance, steatosis and fibrosis, through its impact on gut microbiota composition [31,32].

This study aims to evaluate the effects of melatonin and *A. muciniphila*, administered either alone or in combination, on metabolic parameters, liver disease severity, gut barrier integrity and gut microbiota composition and functionality in an in vivo model of MASLD-associated liver fibrosis.

Overall, melatonin and/or *A. muciniphila* administration induced only modest improvements in hepatic and systemic parameters in this MASLD-associated liver fibrosis model. Although some trends were observed, such as lower serum cholesterol levels and liver weight in *A. muciniphila*-treated groups and subtle reductions in transaminases in the WDMA group, these effects did not translate into consistent or robust improvements across biochemical, histological or fibrotic endpoints. This contrasts with previous studies reporting more pronounced metabolic and hepatic benefits of melatonin [33,34] or *A. muciniphila* supplementation [31,32,35,36], suggesting that, in our experimental setting, maintaining Western diet feeding, together with the relatively short intervention period (four weeks), may have limited the extent of hepatic recovery once liver damage was already established.

At the histological level, hepatocellular ballooning was the only feature consistently ameliorated by treatment. This observation is in line with previous studies reporting improvements in ballooning in response to melatonin [37,38] and describing a negative association between Verrucomicrobiales abundance and ballooning in NASH patients [39] and suggests that melatonin and *A. muciniphila* may preferentially influence specific components of hepatocellular injury rather than advanced structural damage. In parallel, the downregulation of profibrogenic and inflammatory genes, such as *Timp1*, *Tlr4* or *Tgfb1*, in response to melatonin and/or *A. muciniphila* aligns with previous studies [32,40,41] and may reflect early molecular adaptations that were insufficient to elicit detectable histological improvement within the timeframe of this study. Together, these findings support the idea that, while short-term intervention can induce molecular and cellular changes, longer or earlier treatments, and potentially optimised dosing or combination strategies, may be required to achieve overt hepatic protection in MASLD under sustained dietary challenge.

In contrast to the limited hepatic effects, intestinal readouts appeared more responsive to the interventions. Melatonin tended to restore *Cldn1* expression, consistent with its previously reported ability to upregulate genes involved in epithelial barrier maintenance [42,43], while *A. muciniphila* significantly increased *Muc2* expression and showed a trend towards increased *Tjp1*, in line with its capacity to reinforce mucus production and barrier-related mechanisms [35,44]. These differences between intestinal and hepatic responses suggest that, in our model, melatonin and *A. muciniphila* had already elicited measurable effects at the intestinal level, whereas corresponding hepatic improvements were still not detectable, particularly under sustained dietary challenge, thereby positioning the intestine and the gut microbiota as the earliest responsive targets of these interventions.

Gut microbiota composition was markedly altered by WD feeding in our MASLD–fibrosis model, with shifts in several taxa previously implicated in MASLD and liver fibrosis [31,45,46]. Melatonin and *A. muciniphila* administration produced modest but directionally consistent effects on gut microbiota composition, partially counteracting WD-induced disturbances, attenuating the increase in harmful taxa and promoting the enrichment of beneficial ones.

Among the genera enriched in the WD group, *Blautia* and *Alistipes* stood out for their consistent associations with adverse metabolic and hepatic outcomes. *Blautia* abundance correlated positively with serum cholesterol, ALT and *Timp1* expression, in line with previous studies linking this genus to dyslipidaemia [47,48] and hepatocellular injury [49]. *Alistipes* also showed positive correlations with cholesterol and *Timp1*, reinforcing its potential deleterious role in advanced stages of disease [50]. Neither melatonin nor *A. muciniphila* significantly reduced their abundance, which could indicate that these taxa may represent resilient features of WD-induced dysbiosis, although a non-significant trend towards lower *Alistipes* levels was observed with melatonin and towards lower *Blautia* with *A. muciniphila*. In addition, *Faecalibaculum* was also increased, consistent with

 doi:10.20944/preprints202602.0461.v1

associations with MASLD pathogenesis [51], obesity, gut inflammation, endotoxaemia and oxidative stress [52]. Its negative correlations with several dicarboxylic acids and mevalonate pathway intermediates suggest links with altered lipid [53] and cholesterol metabolism [54], supporting its contribution to metabolic and oxidative stress-related processes [55].

Both *Intestinimonas* and *Lachnoclostridium* were increased in the WD group and positively associated with cholesterol, glucose and metabolites such as hydroferulic acid, tromethamine and N-formylmethionine, the latter a pro-inflammatory bacterial peptide, reinforcing their reported involvement in metabolic and immune dysregulation [56,57]. Notably, *Intestinimonas* tended to decrease under the combined treatment, which could be beneficial given the links of these genera to dyslipidaemia, impaired glucose metabolism, oxidative stress and inflammation [58,59].

Other genera with potential harmful effects also showed increased abundance in the liver fibrosis model. *Lactococcus* and *Parasutterella* were enriched in WD-fed groups and showed negative associations with dicarboxylic acids and other metabolites linked to lipid metabolism and oxidative stress. While previous studies reported a reduction of *Lactococcus* after *A. muciniphila* [60] or antioxidant treatments [31,61], in the liver fibrosis model neither melatonin nor *A. muciniphila* significantly modified its abundance. *Tuzzerella*, another genus associated with metabolic stress, also remained elevated despite interventions. It displayed negative correlations with metabolites related to redox balance and energy metabolism, including antioxidants and TCA cycle intermediates, suggesting a potential involvement in oxidative stress and mitochondrial dysfunction.

Conversely, genera typically considered beneficial, such as *Muribaculum* and *Lactobacillus*, were reduced in WD-fed animals. *Lactobacillus* correlated negatively with inflammatory and fibrogenic gene expression. Given its well-described anti-inflammatory properties [62,63], its depletion in WD-fed animals is consistent with the pro-inflammatory environment of MASLD, where protective mechanisms against inflammation appear diminished. *Muribaculum* abundance correlated negatively with cholesterol and glucose and faecal concentrations of hydroferulic acid and N-formylmethionine, and positively with intestinal barrier gene expression (*Tjp1*) and faecal concentrations of 2-hydroxybutyric acid, consistent with its protective metabolic profile and its beneficial role in maintaining intestinal barrier integrity [64,65]. Aligning with reports of increased *Muribaculum* following probiotic [66] and antioxidant interventions [67], including studies with *A. muciniphila* [65], this genus showed a tendency towards restoration in the combined treatment group (WDMA).

Notably, melatonin and *A. muciniphila* did induce favourable shifts in other taxa. *Eisenbergiella*, which was enriched in the WDA and WDMA groups, correlated negatively with multiple metabolites linked to energy metabolism and oxidative stress and has been reported to be reduced in MASLD patients [68], suggesting a shift towards relative abundance values similar to the control group, possibly linked to a healthier profile.

In our study, *Odoribacter* abundance showed a downward trend across treatment groups. While previous reports have associated *Odoribacter* restoration after probiotic or antioxidant interventions with improved metabolic and inflammatory profiles [69,70], in our model, we observed other features of the gut microbiota composition and metabolism that suggest the initiation of an inflammatory remodelling process. Similarly, *Oscillibacter*, although frequently increased in MASLD models [71,72], was reduced in our WD-fed mice despite its positive correlation with serum triglyceride levels. Taken together, these findings reflect a context-dependent role of these genera in MASLD pathogenesis.

Regarding gut microbiota functionality, WD feeding led to increased levels of choline, muricholic acid and phosphocholine. Choline has been associated with steatosis, fibrosis and NASH risk [73,74], likely reflecting alterations in phospholipid metabolism and hepatic lipid export mechanisms. Muricholic acid elevation may reflect an altered bile acid profile consistent with MASLD-associated metabolic dysregulation. Importantly, tauro-β-muricholic acid, an farnesoid X receptor antagonist, tended to decrease in the WDA group, in line with previous studies [75] where *A. muciniphila* reduced this bile acid and improved disease features [76,77]. Phosphocholine, involved in very low-density lipoprotein–associated triglycerides synthesis, was also elevated, consistent with reports linking this metabolite to increased fibrosis severity [78].

 doi:10.20944/preprints202602.0461.v1

Microbiota-derived tryptophan metabolites were particularly affected. Indole-3-acetic acid, consistently reduced in MASLD [79,80], showed a trend towards recovery in WDA and WDMA groups, suggesting partial restoration of microbial metabolic activity and a shift to a more favourable environment, in agreement with its reported therapeutic effects, including reduced oxidative stress and inflammation, improved insulin resistance and lipid metabolism, and attenuation of steatosis and ballooning [79,80]. Indole-3-glyoxylic acid, another tryptophan-derived microbial metabolite with reported benefits on intestinal barrier integrity and inflammation control [81], was significantly decreased in our fibrosis model, consistent with the loss of a protective factor.

Isocitric acid, often elevated in MASLD, particularly in advanced disease stages [82,83], was significantly decreased in the WDA group, suggesting a treatment-related improvement. Sebacic acid, previously linked to insulin resistance and dyslipidaemia [84], was significantly reduced by the combined treatment (WDMA), and its inverse correlations with hepatic inflammation and fibrosis markers support a possible amelioration of disease severity.

Finally, phenylacetylglutamine, recognised as a hallmark metabolite of MASLD [85], was markedly increased in the liver fibrosis model. This amino acid–derived compound has been associated with adverse outcomes in cardiovascular and neurodegenerative diseases [86,87], while its reduction after BMI loss in obesity supports a link with metabolic improvement [88]. Interestingly, melatonin-treated animals (WDM and WDMA groups) exhibited elevated levels, a novel and unexpected finding not previously reported, which may point to complex or context-dependent effects of the treatment.

Our findings provide new insights into the multifactorial nature of MASLD and the complex interplay between gut microbiota, microbial- and host-derived metabolites and key molecular pathways involved in the pathogenesis of liver disease. The integrative analysis of gut microbiota composition, faecal metabolome, gut and liver gene expression, represents a noteworthy aspect of this study, as it enabled the identification of specific microbial and metabolic signatures associated with disease progression, which may serve as non-invasive biomarkers for disease monitoring or as therapeutic targets. Importantly, the melatonin and *A. muciniphila* administration, alone or in combination, induced measurable changes in the gut microbiota composition, faecal metabolome and intestinal gene expression, establishing microbial, metabolomic and intestinal signatures that could serve as a foundation for future studies exploring their potential as adjunctive therapies to modulate the gut-liver axis in MASLD.

However, a number of limitations must be acknowledged. Melatonin and/or *A. muciniphila* produced minimal changes in hepatic and systemic parameters, likely reflecting the short treatment duration (four weeks) and the continued exposure to Western diet, which may have limited their capacity to improve liver injury. Nevertheless, consistent trends in gut microbiota composition and function, as well as at the molecular level, including partial modulation of inflammatory and profibrogenic genes and restoration of barrier-related gene expression, indicate that these interventions elicit measurable effects in the gut and microbiota, providing a foundation for future adjunctive strategies targeting the gut–liver axis, particularly if applied earlier or under more favourable conditions.

Further research is warranted to elucidate the specific mechanisms through which *A. muciniphila* and melatonin exert their effects and to explore potential synergistic interactions. Extending the duration or initiating interventions earlier, as well as investigating other relevant tissues, such as adipose tissue or the gut–brain axis, may provide a more comprehensive understanding of their systemic impact. Ultimately, validation in human cohorts will be essential to confirm the identified microbial and metabolomic signatures and to assess the translational potential of these strategies as adjunctive approaches for MASLD management.

5. Conclusions

In conclusion, our results indicate that melatonin and *A. muciniphila*, administered alone or in combination, profoundly reshape gut microbiota composition and functionality, and modulate

 doi:10.20944/preprints202602.0461.v1

intestinal gene expression, whereas effects on hepatic parameters reflected only initial changes. These findings provide new insights into the interactions between the gut microbiota, microbial and host-derived metabolites and the intestinal environment in MASLD. The integrative multi-omic approach allowed the identification of microbial and metabolic signatures, offering a foundation for future studies exploring their potential as biomarkers or therapeutic targets. Although improvements in liver function and histology were limited under fibrotic conditions, the observed modulation of the gut–liver axis suggests that targeting the microbiota and intestinal environment may represent a promising starting point for adjunctive therapies. Further research should assess longer or earlier interventions, dose-response effects and combined strategies to maximise therapeutic efficacy and clarify the mechanisms underlying gut–liver crosstalk in MASLD.

Supplementary Materials: The following supporting information can be downloaded at the website of this paper posted on Preprints.org. Table S1: Probes used for mRNA expression analyses by RT-qPCR, Table S2: Biochemical determinations after 8 weeks of WD feeding, Figure S1: Haematoxylin and eosin-stained liver sections (x10), Figure S2: Masson's trichrome-stained liver sections (x10), Figure S3: Assessment of the comparability of control subgroups (C, CM, CA and CMA) for the analysed parameters using one-way ANOVA, Figure S4: Analysis of gut microbiota α-diversity measured by the Shannon and Simpson indices, Figure S5: Correlation analysis. Heatmaps showing Spearman correlations between A) serum biochemical parameters and faecal metabolites, B) hepatic gene expression and bacterial genera, C) hepatic gene expression and faecal metabolites, and D) intestinal gene expression and bacterial genera. Each square represents the Spearman's correlation coefficient ($q < 0.05$). Red and blue cells represent positive and negative correlations, respectively. White crosses designate the level of significance: + $q < 0.05$; ++ $q < 0.01$; +++ $q < 0.001$.

Author Contributions: Conceptualization, M.J.-F., J.L.M., S.M.-F., E.N., M.V.G.-M. and S.S.-C.; Methodology: M.V.G.-M. and S.S.-C.; Software, A.G.-R., B.SM., S.R.-S. and M.J.-F.; Validation, B.SM., J.L.M., M.V.G.-M. and S.S.-C.; Formal analysis, A.G.-R., B.SM., S.R.-S., M.J.-F., E.N., M.V.G.-M. and S.S.-C.; Investigation, A.G.-R., B.SM., S.R.-S., M.J.-F., J.L.M., S.M.-F., E.N., M.V.G.-M. and S.S.-C.; Resources, J.L.M., S.M.-F., M.V.G.-M. and S.S.-C.; Data curation: S.R.-S., M.J.-F., E.N., M.V.G.-M. and S.S.-C; Writing - Original Draft Preparation, A.G.-R., E.N., M.V.G.-M. and S.S.-C.; Writing - Review & Editing: A.G.-R., B.SM., S.R.-S., M.J.-F., J.L.M., S.M.-F., E.N., M.V.G.-M. and S.S.-C.; Visualization, A.G.-R., E.N., M.V.G.-M. and S.S.-C.; Supervision: E.N., M.V.G.-M. and S.S.-C.; Project administration, E.N., M.V.G.-M. and S.S.-C.; Funding acquisition: S.S.-C. All authors have read and agreed to the published version of the manuscript.

Funding: This work was supported by grants from Ministerio de Ciencia e Innovación (PID2020-.120363RB-I00), Junta de Castilla y León and the European Regional Development Fund (GRS2126/A/2020 and LE017-P20) and Instituto de Salud Carlos III (ISCIII) (PI20/00690) co-funded by the European Union. CIBERehd is funded by the ISCIII. AGR was supported by a fellowship from Ministerio de Educación (FPU22/02734). MJF was supported by a fellowship from Ministerio de Educación (FPU18/06257). SRS was supported by a Fellowship to Finance the Predoctoral Recruitment of Research Personnel by the Junta of Castilla y Leon.

Institutional Review Board Statement: The animal study protocol was approved by the Institutional Animal Care and Use Committee of the University of León (OEBA-ULE-004-2021) on 22nd March 2021, and subsequently authorised by the competent authority, the Junta de Castilla y León.

Conflicts of Interest: The authors declare no conflicts of interest.

References

1. Chan, W.-K.; Chuah, K.-H.; Rajaram, R.B.; Lim, L.-L.; Ratnasingam, J.; Vethakkan, S.R. Metabolic Dysfunction-Associated Steatotic Liver Disease (MASLD): A State-of-the-Art Review. *J Obes Metab Syndr* **2023**, *32*, 197–213.
2. Miao, L.; Targher, G.; Byrne, C.D.; Cao, Y.-Y.; Zheng, M.-H. Current Status and Future Trends of the Global Burden of MASLD. *Trends Endocrinol Metab* **2024**, *35*, 697–707.

 doi:10.20944/preprints202602.0461.v1

3. Ha, S.; Wai-Sun Wong, V.; Zhang, X.; Yu, J. Interplay between Gut Microbiome, Host Genetic and Epigenetic Modifications in MASLD and MASLD-Related Hepatocellular Carcinoma. *Gut* **2024**, *0*, 1-12.
4. Tanwar, S.; Rhodes, F.; Srivastava, A.; Trembling, P.M.; Rosenberg, W.M. Inflammation and Fibrosis in Chronic Liver Diseases Including Non-Alcoholic Fatty Liver Disease and Hepatitis C. *World J Gastroenterol* **2020**, *26*, 109–133.
5. Aydın, M.M.; Akçalı, K.C. Liver Fibrosis. *Turk J Gastroenterol* **2018**, *29*, 14–21.
6. Mitra, S.; De, A.; Chowdhury, A. Epidemiology of Non-Alcoholic and Alcoholic Fatty Liver Diseases. *Transl Gastroenterol Hepatol* **2020**, *5*, 16.
7. Saenz, E.; Montagut, N.E.; Wang, B.; Stein-Thöringer, C.; Wang, K.; Weng, H.; Ebert, M.; Schneider, K.M.; Li, L.; Teufel, A. Manipulating the Gut Microbiome to Alleviate Steatotic Liver Disease: Current Progress and Challenges. *Engineering* **2024**, *40*, 51–60.
8. Martin-Grau, M.; Monleón, D. The Role of Microbiota-Related Co-Metabolites in MASLD Progression: A Narrative Review. *Curr Issues Mol Biol* **2024**, *46*, 6377–6389.
9. Zhang, R.; Yan, Z.; Zhong, H.; Luo, R.; Liu, W.; Xiong, S.; Liu, Q.; Liu, M. Gut Microbial Metabolites in MASLD: Implications of Mitochondrial Dysfunction in the Pathogenesis and Treatment. *Hepatol Commun* **2024**, *8*, e0484.
10. Benedé-Ubieto, R.; Cubero, F.J.; Nevzorova, Y.A. Breaking the Barriers: The Role of Gut Homeostasis in Metabolic-Associated Steatotic Liver Disease (MASLD). *Gut Microbes* **2024**, *16*, 2331460.
11. Vallianou, N.G.; Kounatidis, D.; Psallida, S.; Vythoulkas-Biotis, N.; Adamou, A.; Zachariadou, T.; Kargioti, S.; Karampela, I.; Dalamaga, M. NAFLD/MASLD and the Gut–Liver Axis: From Pathogenesis to Treatment Options. *Metabolites* **2024**, *14*, 366.
12. Kim, J.I.; Cheon, H.G. Melatonin Ameliorates Hepatic Fibrosis via the Melatonin Receptor 2-Mediated Upregulation of BMAL1 and Anti-Oxidative Enzymes. *Eur J Pharmacol* **2024**, *966*, 176337.
13. Ahmand, S.B.; Ali, A.; Bilal, M.; Rashid, S.M.; Wani, A.B.; Bhat, R.R.; Rehman, M.U. Melatonin and Health: Insights of Melatonin Action, Biological Functions, and Associated Disorders. *Cell Mol Neurobiol* **2023**, *43*, 2437-2458.
14. Iesanu, M.I.; Zahiu, C.D.M.; Dogaru, I.-A.; Chitimus, D.M.; Pircalabioru, G.G.; Voiculescu, S.E.; Isac, S.; Galos, F.; Pavel, B.; O'Mahony, S.M.; et al. Melatonin–Microbiome Two-Sided Interaction in Dysbiosis-Associated Conditions. *Antioxidants* **2022**, *11*, 2244.
15. LeFort, K.R.; Rungratanawanich, W.; Song, B.-J. Melatonin Prevents Alcohol- and Metabolic Dysfunction-Associated Steatotic Liver Disease by Mitigating Gut Dysbiosis, Intestinal Barrier Dysfunction, and Endotoxemia. *Antioxidants* **2023**, *13*, 43.
16. Han, Y.; Li, L.; Wang, B. Role of Akkermansia Muciniphila in the Development of Nonalcoholic Fatty Liver Disease: Current Knowledge and Perspectives. *Front Med* **2022**, *16*, 667–685.
17. Derrien, M.; Vaughan, E.E.; Plugge, C.M.; de Vos, W.M. Akkermansia Muciniphila Gen. Nov., Sp. Nov., a Human Intestinal Mucin-Degrading Bacterium. *Int J Syst Evol Microbiol* **2004**, *54*, 1469–1476.
18. Pai, R.K. NAFLD Histology: A Critical Review and Comparison of Scoring Systems. *Curr Hepatology Rep* **2019**, *18*, 473–481.
19. Porras, D.; Nistal, E.; Martínez-Flórez, S.; Pisonero-Vaquero, S.; Olcoz, J.L.; Jover, R.; González-Gallego, J.; García-Mediavilla, M.V.; Sánchez-Campos, S. Protective Effect of Quercetin on High-Fat Diet-Induced Non-Alcoholic Fatty Liver Disease in Mice Is Mediated by Modulating Intestinal Microbiota Imbalance and Related Gut-Liver Axis Activation. *Free Radic Biol Med* **2017**, *102*, 188–202.
20. Porras, D.; Nistal, E.; Martínez-Flórez, S.; Olcoz, J.L.; Jover, R.; Jorquera, F.; González-Gallego, J.; García-Mediavilla, M.V.; Sánchez-Campos, S. Functional Interactions between Gut Microbiota Transplantation, Quercetin, and High-Fat Diet Determine Non-Alcoholic Fatty Liver Disease Development in Germ-Free Mice. *Mol Nutr Food Res* **2019**, *63*, 1800930.
21. Babraham Bioinformatics. *FastQC*, version 0.11.9; A quality control tool for high throughput sequence data; Babraham Institute: United Kingdom, 2020.
22. Caporaso, J.G.; Kuczynski, J.; Stombaugh, J.; Bittinger, K.; Bushman, F.D.; Costello, E.K.; Fierer, N.; Peña, A.G.; Goodrich, J.K.; Gordon, J.I.; et al. QIIME Allows Analysis of High-Throughput Community Sequencing Data. *Nat Methods* **2010**, *7*, 335–336.

 doi:10.20944/preprints202602.0461.v1

23. Callahan, B.J.; McMurdie, P.J.; Rosen, M.J.; Han, A.W.; Johnson, A.J.A.; Holmes, S.P. DADA2: High-Resolution Sample Inference from Illumina Amplicon Data. *Nat Methods* **2016**, *13*, 581–583.
24. Vidal-Cevallos, P.; Sorroza-Martínez, A.P.; Chávez-Tapia, N.C.; Uribe, M.; Montalvo-Javé, E.E.; Nuño-Lámbarri, N. The Relationship between Pathogenesis and Possible Treatments for the MASLD-Cirrhosis Spectrum. *Int J Mol Sci* **2024**, *25*, 4397.
25. Zazueta, A.; Valenzuela-Pérez, L.; Ortiz-López, N.; Pinto-León, A.; Torres, V.; Guiñez, D.; Aliaga, N.; Merino, P.; Sandoval, A.; Covarrubias, N.; et al. Alteration of Gut Microbiota Composition in the Progression of Liver Damage in Patients with Metabolic Dysfunction-Associated Steatotic Liver Disease (MASLD). *Int J Mol Sci* **2024**, *25*, 4387.
26. Soto, A.; Spongberg, C.; Martinino, A.; Giovinazzo, F. Exploring the Multifaceted Landscape of MASLD: A Comprehensive Synthesis of Recent Studies, from Pathophysiology to Organoids and Beyond. *Biomedicines* **2024**, *12*, 397.
27. Guan, Q.; Wang, Z.; Cao, J.; Dong, Y.; Chen, Y. Mechanisms of Melatonin in Obesity: A Review. *Int J Mol Sci* **2021**, *23*, 218.
28. Yin, J.; Li, Y.; Han, H.; Chen, S.; Gao, J.; Liu, G.; Wu, X.; Deng, J.; Yu, Q.; Huang, X.; et al. Melatonin Reprogramming of Gut Microbiota Improves Lipid Dysmetabolism in High-Fat Diet-Fed Mice. *J Pineal Res* **2018**, *65*, e12524.
29. Hong, F.; Pan, S.; Xu, P.; Xue, T.; Wang, J.; Guo, Y.; Jia, L.; Qiao, X.; Li, L.; Zhai, Y. Melatonin Orchestrates Lipid Homeostasis through the Hepatointestinal Circadian Clock and Microbiota during Constant Light Exposure. *Cells* **2020**, *9*, 489.
30. Xu, P.; Wang, J.; Hong, F.; Wang, S.; Jin, X.; Xue, T.; Jia, L.; Zhai, Y. Melatonin Prevents Obesity through Modulation of Gut Microbiota in Mice. *J Pineal Res* **2017**, *62*, e12399.
31. Juárez-Fernández, M.; Porras, D.; Petrov, P.; Román-Sagüillo, S.; García-Mediavilla, M.V.; Soluyanova, P.; Martínez-Flórez, S.; González-Gallego, J.; Nistal, E.; Jover, R.; et al. The Synbiotic Combination of Akkermansia Muciniphila and Quercetin Ameliorates Early Obesity and NAFLD through Gut Microbiota Reshaping and Bile Acid Metabolism Modulation. *Antioxidants* **2021**, *10*, 2001.
32. Keshavarz Azizi Raftar, S.; Ashrafian, F.; Yadegar, A.; Lari, A.; Moradi, H.R.; Shahriary, A.; Azimirad, M.; Alavifard, H.; Mohsenifar, Z.; Davari, M.; et al. The Protective Effects of Live and Pasteurized Akkermansia Muciniphila and Its Extracellular Vesicles against HFD/CCl4-Induced Liver Injury. *Microbiol Spectr 9*, e00484-21.
33. 33. Cinar, C.; Altinoz, E.; Elbe, H.; Bicer, Y.; Cetinavci, D.; Ozturk, I.; Colak, T. Therapeutic Effect of Melatonin on CCl4-Induced Fibrotic Liver Model by Modulating Oxidative Stress, Inflammation, and TGF-B1 Signaling Pathway in Pinealectomized Rats. *Inflammation* **2025**, 48, 1093-1108.
34. 34. Sun, H.; Wang, X.; Chen, J.; Song, K.; Gusdon A.M.; Li, L.; Bu, L.; Qu, S. Melatonin Improves Non-Alcoholic Fatty Liver Disease via MAPK-JNK/P38 Signaling in High-Fat-Diet-Induced Obese Mice. *Lipids Health Dis* **2016**, *15*, 202.
35. Wu, W.; Lv, L.; Shi, D.; Ye, J.; Fang, D.; Guo, F.; Li, Y.; He, X.; Li, L. Protective Effect of Akkermansia Muciniphila against Immune-Mediated Liver Injury in a Mouse Model. *Front Microbiol* **2017**, *8*, 1804.
36. Qu, D.; Chen, M.; Zhu, H.; Liu, X.; Cui, Y.; Zhou, W.; Zhang, M. *Akkermansia Muciniphila* and Its Outer Membrane Protein Amuc_1100 Prevent High-Fat Diet-Induced Nonalcoholic Fatty Liver Disease in Mice. *Biochem Biophys Res Commun* **2023**, *684*, 149131.
37. Saha, M.; Manna, K.; Saha, K.D. Melatonin Suppresses NLRP3 Inflammasome Activation via TLR4/NF-κB and P2X7R Signaling in High-Fat Diet-Induced Murine NASH Model. *J Inflamm Res* **2022**, *15*, 3235–3258.
38. El-Sayed, S.M.; El-Sayed, G.A.; Mansour, M.A; Ahmed, H.E.; Kamar, S.A. A Comparative Study on the Effect of Melatonin and Orlistat Combination versus Orlistat Alone on High Fat Diet-Induced Hepatic Changes in the Adult Male Albino Rats (a Histological and Morphometric Study). *Ultrastruc Pathol* **2025**, *49*, 20–38.
39. Machado-de Oliveira, J.; Lima-Pace, F.H.; de Faria-Ghetti, F.; Bastos-Dias-Barbosa, K.V.; Evangelista-Cesar, D; Fonseca-Chebli, J.M.; Villela-Vieira-de Castro-Ferreira, L.E. Non-Alcoholic Steatohepatitis: Comparison of Intestinal Microbiota between Different Metabolic Profiles. A Pilot Study. *J Gastrointestin Liver Dis* **2020**, *29*, 369–376.

 doi:10.20944/preprints202602.0461.v1

40. Moraes-Miguel, F.; Nascimiento-Picada, J.; Bondan-da Silva, J.; Gonçalves-Schemitt, E.; Raskopt-Colares, J.; Minuzzo-Hartmann, R.; Marroni, C.A.; Possa-Marroni, N. Melatonin Attenuates Inflammation, Oxidative Stress, and DNA Damage in Mice with Nonalcoholic Steatohepatitis Induced by a Methionine- and Choline-Deficient Diet. *Inflammation* **2022**, *45*, 1968–1984.
41. He, F.; Wu, X.; Zhang, Q.; Li, Y.; Ye, Y.; Li, P.; Chen, S.; Peng, Y.; Hardeland, R.; Xia, Y. Bacteriostatic Potential of Melatonin: Therapeutic Standing and Mechanistic Insights. *Front Immunol* **2021**, *12*, 683879.
42. Liu, S.; Kang, W.; Mao, X.; Ge, L.; Du, H.; Li, J.; Hou, L.; Liu, D.; Yin, Y.; Liu, Y.; et al. Melatonin Mitigates Aflatoxin B1-Induced Liver Injury via Modulation of Gut Microbiota/Intestinal FXR/Liver TLR4 Signaling Axis in Mice. *J Pineal Res* **2022**, *73*, e12812.
43. Gao, T.; Wang, Z.; Dong, Y.; Cao, J.; Chen, Y. Melatonin-Mediated Colonic Microbiota Metabolite Butyrate Prevents Acute Sleep Deprivation-Induced Colitis in Mice. *Int J Mol Sci* **2021**, *22*, 11894.
44. Martin-Gallausiaux, C.; Garcia-Weber, D.; Lashermes, A.; Larraufie, P.; Marinelli, L.; Teixeira, V.; Rolland, A.; Béguet-Crespel, F.; Brochard, V.; Quatremare, T.; et al. Akkermansia Muciniphila Upregulates Genes Involved in Maintaining the Intestinal Barrier Function via ADP-Heptose-Dependent Activation of the ALPK1/TIFA Pathway. *Gut Microbes* **2022**, *14*, 2110639.
45. Aron-Wisnewsky, J.; Vigliotti, C.; Witjes, J.; Le, P.; Holleboom, A.G.; Verheij, J.; Nieuwdorp, M.; Clément, K. Gut Microbiota and Human NAFLD: Disentangling Microbial Signatures from Metabolic Disorders. *Nat Rev Gastroenterol Hepatol* **2020**, *17*, 279–297.
46. Li, Z.; Ni, M.; Yu, H.; Wang, L.; Zhou, X.; Chen, T.; Liu, G.; Gao, Y. Gut Microbiota and Liver Fibrosis: One Potential Biomarker for Predicting Liver Fibrosis. *Biomed Res Int* **2020**, *2020*, 3905130.
47. Gong, S.; Ye, T.; Wang, M.; Wang, M.; Li, Y.; Ma, L.; Yang, Y.; Wang, Y.; Zhao, X.; Liu, L.; et al. Traditional Chinese Medicine Formula Kang Shuai Lao Pian Improves Obesity, Gut Dysbiosis, and Fecal Metabolic Disorders in High-Fat Diet-Fed Mice. *Front Pharmacol* **2020**, *11*.
48. Li, X.; Xiao, Y.; Song, L.; Huang, Y.; Chu, Q.; Zhu, S.; Lu, S.; Hou, L.; Li, Z.; Li, J.; et al. Effect of *Lactobacillus Plantarum* HT121 on Serum Lipid Profile, Gut Microbiota, and Liver Transcriptome and Metabolomics in a High-Cholesterol Diet–Induced Hypercholesterolemia Rat Model. *Nutrition* **2020**, *79–80*, 110966.
49. Bao, T.; He, F.; Zhang, X.; Zhu, L.; Wang, Z.; Lu, H.; Wang, T.; Li, Y.; Yang, S.; Wang, H. Inulin Exerts Beneficial Effects on Non-Alcoholic Fatty Liver Disease via Modulating Gut Microbiome and Suppressing the Lipopolysaccharide-Toll-Like Receptor 4-Mψ-Nuclear Factor-κB-Nod-Like Receptor Protein 3 Pathway via Gut-Liver Axis in Mice. *Front Pharmacol* **2020**, *11*.
50. Zhuge, A.; Li, S.; Lou, P.; Wu, W.; Wang, K.; Yuan, Y.; Xia, J.; Li, B.; Li, L. Longitudinal 16S rRNA Sequencing Reveals Relationships among Alterations of Gut Microbiota and Nonalcoholic Fatty Liver Disease Progression in Mice. *Microbiol Spectr 10*, e00047-22.
51. Duan, R.; Huang, K.; Guan, X.; Li, S.; Xia, J.; Shen, M.; Sun, Z.; Yu, Z. Tectorigenin Ameliorated High-Fat Diet-Induced Nonalcoholic Fatty Liver Disease through Anti-Inflammation and Modulating Gut Microbiota in Mice. *Food Chem Toxicol* **2022**, *164*, 112948.
52. Yu, J.; Sun, H.; Yang, Y.; Yan, Y. Sesamolin Alleviates Nonalcoholic Fatty Liver Disease through Modulating Gut Microbiota and Metabolites in High-Fat and High-Fructose Diet-Fed Mice. *Int J Mol Sci* **2022**, *23*, 13853.
53. Ranea-Robles, P.; Houten, S.M. The Biochemistry and Physiology of Long-Chain Dicarboxylic Acid Metabolism. *Biochem J* **2023**, *480*, 607–627.
54. Hashemi, M.; Hoshyar, R.; Ande, S.R.; Chen, Q.M.; Solomon, C.; Zuse, A.; Naderi, M. Mevalonate Cascade and Its Regulation in Cholesterol Metabolism in Different Tissues in Health and Disease. *Curr Mol Pharmacol 10*, 13–26.
55. Jabłońska-Trypuć, A.; Pankiewicz, W.; Czerpak, R. Traumatic Acid Reduces Oxidative Stress and Enhances Collagen Biosynthesis in Cultured Human Skin Fibroblasts. *Lipids* **2016**, *51*, 1021–1035.
56. Kuley, R.; Stultz, R.D.; Duvvuri, B.; Wang, T.; Fritzler, M.J.; Hesselstrand, R.; Nelson, J.L.; Lood, C. N-Formyl Methionine Peptide-Mediated Neutrophil Activation in Systemic Sclerosis. *Front Immunol* **2022**, *12*, 785275.
57. Michailidou, D.; Duvvuri, B.; Kuley, R.; Cuthbertson, D.; Grayson, P.C.; Khalidi, N.A.; Koening, C.L.; Langford, C.A.; McAlear, C.A.; Moreland, L.W.; et al. Neutrophil Activation in Patients with Anti-

 doi:10.20944/preprints202602.0461.v1

Neutrophil Cytoplasmic Autoantibody-Associated Vasculitis and Large-Vessel Vasculitis. *Arthritis ResTher* **2022**, *24*, 160.

58. Sánchez-Medina, A.; Redondo-Puente, M.; Dupak, R.; Bravo-Clemente, L.; Goya, L.; Sarriá, B. Colonic Coffee Phenols Metabolites, Dihydrocaffeic, Dihydroferulic, and Hydroxyhippuric Acids Protect Hepatic Cells from TNF-α-Induced Inflammation and Oxidative Stress. *Int J Mol Sci* **2023**, *24*, 1440.
59. Larrosa, M.; Luceri, C.; Vivoli, E.; Pagliuca, C.; Lodovici, M.; Moneti, G.; Dolara, P. Polyphenol Metabolites from Colonic Microbiota Exert Anti-Inflammatory Activity on Different Inflammation Models. *Mol Nutr Food Res* **2009**, *53*, 1044–1054.
60. Chen, T.; Wang, R.; Duan, Z.; Yuan, X.; Ding, Y.; Feng, Z.; Bu, F.; Liu, L.; Wang, Q.; Zhou, J.; et al. Akkermansia Muciniphila Protects Against Psychological Disorder-Induced Gut Microbiota-Mediated Colonic Mucosal Barrier Damage and Aggravation of Colitis. *Front Cell Infect Microbiol* **2021**, *11*, 723856.
61. Wang, M.; Han, H.; Wan, F.; Zhong, R.; Do, Y.J.; Oh, S.-I.; Lu, X.; Liu, L.; Yi, B.; Zhang, H. Dihydroquercetin Supplementation Improved Hepatic Lipid Dysmetabolism Mediated by Gut Microbiota in High-Fat Diet (HFD)-Fed Mice. *Nutrients* **2022**, *14*, 5214.
62. Carvalho, J.L.; Miranda, M.; Fialho, A.K.; Castro-Faria-Neto, H.; Anatriello, E.; Keller, A.C.; Aimbire, F. Oral Feeding with Probiotic Lactobacillus Rhamnosus Attenuates Cigarette Smoke-Induced COPD in C57Bl/6 Mice: Relevance to Inflammatory Markers in Human Bronchial Epithelial Cells. *PLoS One* **2020**, *15*, e0225560.
63. Wang, K.; Wu, W.; Jiang, X.; Xia, J.; Lv, L.; Li, S.; Zhuge, A.; Wu, Z.; Wang, Q.; Wang, S.; et al. Multi-Omics Analysis Reveals the Protection of Gasdermin D in Concanavalin A-Induced Autoimmune Hepatitis. *Microbiol Spectr* **2022**, *10*, e01717-22.
64. Wan, M.; Li, Q.; Lei, Q.; Zhou, D.; Wang, S. Polyphenols and Polysaccharides from Morus Alba L. Fruit Attenuate High-Fat Diet-Induced Metabolic Syndrome Modifying the Gut Microbiota and Metabolite Profile. *Foods* **2022**, *11*, 1818.
65. Hu, Y.; Zhou, J.; Lin, X. Akkermansia Muciniphila Helps in the Recovery of Lipopolysaccharide-Fed Mice with Mild Intestinal Dysfunction. *Front Microbiol* **2025**, *16*, 1523742.
66. Li, L.; Wu, L.; Jiang, T.; Liang, T.; Yang, L.; Li, Y.; Gao, H.; Zhang, J.; Xie, X.; Wu, Q. Lactiplantibacillus Plantarum 124 Modulates Sleep Deprivation-Associated Markers of Intestinal Barrier Dysfunction in Mice in Conjunction with the Regulation of Gut Microbiota. *Nutrients* **2023**, *15*, 4002.
67. Wang, L.; Jiang, Y.; Yu, Q.; Xiao, C.; Sun, J.; Weng, L.; Qiu, Y. Gentiopicroside Improves High-Fat Diet-Induced NAFLD in Association with Modulation of Host Serum Metabolome and Gut Microbiome in Mice. *Front Microbiol* **2023**, *14*, 1145430.
68. Rodriguez-Diaz, C.; Taminiau, B.; García-García, A.; Cueto, A.; Robles-Díaz, M.; Ortega-Alonso, A.; Martín-Reyes, F.; Daube, G.; Sanabria-Cabrera, J.; Jimenez-Perez, M.; et al. Microbiota Diversity in Nonalcoholic Fatty Liver Disease and in Drug-Induced Liver Injury. *Pharmacol Res* **2022**, *182*, 106348.
69. Bacil, G.P.; Romualdo, G.R.; Rodrigues, J.; Barbisan, L.F. Indole-3-Carbinol and Chlorogenic Acid Combination Modulates Gut Microbiome and Attenuates Nonalcoholic Steatohepatitis in a Murine Model. *Food Res Int* **2023**, *174*, 113513.
70. Ran, X.; Wang, Y.; Li, S.; Dai, C. Effects of Bifidobacterium and Rosuvastatin on Metabolic-Associated Fatty Liver Disease via the Gut–Liver Axis. *Lipids Health Dis* **2024**, *23*, 401.
71. Gao, W.; Chen, X.; Wu, S.; Jin, L.; Chen, X.; Mao, G.; Wan, X.; Xing, W. Monascus Red Pigments Alleviate High-Fat and High-Sugar Diet-Induced NAFLD in Mice by Modulating the Gut Microbiota and Metabolites. *Food Sci Nutr* **2024**, *12*, 5762–5775.
72. Zhou, D.; Zhang, J.; Xiao, C.; Mo, C.; Ding, B.-S. Trimethylamine-N-Oxide (TMAO) Mediates the Crosstalk between the Gut Microbiota and Hepatic Vascular Niche to Alleviate Liver Fibrosis in Nonalcoholic Steatohepatitis. *Front Immunol* **2022**, *13*, 964477.
73. León-Mimila, P.; Villamil-Ramírez, H.; Li, X.S.; Shih, D.M.; Hui, S.T.; Ocampo-Medina, E.; López-Contreras, B.; Morán-Ramos, S.; Olivares-Arevalo, M.; Grandini-Rosales, P.; et al. Trimethylamine N-Oxide Levels Are Associated with NASH in Obese Subjects with Type 2 Diabetes. *Diabetes Metab* **2021**, *47*, 101183.

 doi:10.20944/preprints202602.0461.v1

74. Imajo, K.; Fujita, K.; Yoneda, M.; Shinohara, Y.; Suzuki, K.; Mawatari, H.; Takahashi, J.; Nozaki, Y.; Sumida, Y.; Kirikoshi, H.; et al. Plasma Free Choline Is a Novel Non-Invasive Biomarker for Early-Stage Non-Alcoholic Steatohepatitis: A Multi-Center Validation Study. *Hepatol Res* **2012**, *42*, 757–766.
75. Luo, Y.; Peng, S.; Cheng, J.; Yang, H.; Lin, L.; Yang, G.; Jin, Y.; Wang, Q.; Wen, Z. Chitosan-Stabilized Selenium Nanoparticles Alleviate High-Fat Diet-Induced Non-Alcoholic Fatty Liver Disease (NAFLD) by Modulating the Gut Barrier Function and Microbiota. *J Funct Biomater* **2024**, *15*, 236.
76. Wang, J.; Zang, J.; Yu, Y.; Liu, Y.; Cao, H.; Guo, R.; Zhang, L.; Liu, M.; Zhang, Z.; Li, X.; et al. Lingguizhugan Oral Solution Alleviates MASLD by Regulating Bile Acids Metabolism and the Gut Microbiota through Activating FXR/TGR5 Signaling Pathways. *Front Pharmacol* **2024**, *15*, 1426049.
77. Yue, H.; Jia, M.; Li, B.; Zong, A.; Du, F.; Xu, T. Medium Chain Triglycerides Alleviate Non-Alcoholic Fatty Liver Disease through Bile Acid-Mediated FXR Signaling Pathway: A Comparative Study with Common Vegetable Edible Oils. *J Food Sci* **2024**, *89*, 10171–10180.
78. Gaggini, M.; Carli, F.; Rosso, C.; Younes, R.; D'Aurizio, R.; Bugianesi, E.; Gastaldelli, A. Altered Metabolic Profile and Adipocyte Insulin Resistance Mark Severe Liver Fibrosis in Patients with Chronic Liver Disease. *Int J Mol Sci* **2019**, *20*, 6333.
79. Ding, Y.; Yanagi, K.; Yang, F.; Callaway, E.; Cheng, C.; Hensel, M.E.; Menon, R.; Alaniz, R.C.; Lee, K.; Jayaraman, A. Oral Supplementation of Gut Microbial Metabolite Indole-3-Acetate Alleviates Diet-Induced Steatosis and Inflammation in Mice. *eLife* **2024**, *13*, 87458.
80. Min, B.H.; Devi, S.; Kwon, G.H.; Gupta, H.; Jeong, J.J.; Sharma, S.P.; Won, S.M.; Oh, K.K.; Yoon, S.J.; Park, H.J.; et al. Gut Microbiota-Derived Indole Compounds Attenuate Metabolic Dysfunction-Associated Steatotic Liver Disease by Improving Fat Metabolism and Inflammation. *Gut Microbes* **2024**, *16*, 2307568.
81. Ouyang, C.; Liu, P.; Liu, Y.; Lan, J.; Liu, Q. Metabolites Mediate the Causal Associations between Gut Microbiota and NAFLD: A Mendelian Randomization Study. *BMC Gastroenterol* **2024**, *24*, 244.
82. Chashmniam, S.; Ghafourpour, M.; Farimani, A.R.; Gholami, A.; Ghoochani, B.F.N.M. Metabolomic Biomarkers in the Diagnosis of Non-Alcoholic Fatty Liver Disease. *Hepat Mon* **2019**, *19*, e92244.
83. Ji, M.; Jo, Y.; Choi, S.J.; Kim, S.M.; Kim, K.K.; Oh, B.C.; Ryu, D.; Paik, M.J.; Lee, D.H. Plasma Metabolomics and Machine Learning-Driven Novel Diagnostic Signature for Non-Alcoholic Steatohepatitis. *Biomedicines* **2022**, *10*, 1669.
84. Aggarwal, H.; Pathak, P.; Kumar, Y.; Jagavelu, K.; Dikshit, M. Modulation of Insulin Resistance, Dyslipidemia and Serum Metabolome in iNOS Knockout Mice Following Treatment with Nitrite, Metformin, Pioglitazone, and a Combination of Ampicillin and Neomycin. *Int J Mol Sci* **2022**, *23*, 195.
85. Oh, K.K.; Gupta, H.; Min, B.H.; Ganesan, R.; Sharma, S.P.; Won, S.M.; Jeong, J.J.; Lee, S.B.; Cha, M.G.; Kwon, G.H.; et al. The Identification of Metabolites from Gut Microbiota in NAFLD via Network Pharmacology. *Sci Rep* **2023**, *13*, 724.
86. Cirstea, M.S.; Yu, A.C.; Golz, E.; Sundvick, K.; Kliger, D.; Radisavljevic, N.; Foulger, L.H.; Mackenzie, M.; Huan, T.; Finlay, B.B.; et al. Microbiota Composition and Metabolism Are Associated With Gut Function in Parkinson's Disease. *Mov Disord* **2020**, *35*, 1208–1217.
87. Nemet, I.; Saha, P.P.; Gupta, N.; Fischbach, M.A.; DiDonato, J.A.; Hazen, S.L. A Cardiovascular Disease-Linked Gut Microbial Metabolite Acts via Adrenergic Receptors. *Cell* **2020**, *180*, 862-877.
88. Barton, W.; Cronin, O.; García-Pérez, I.; Wiston, R.; Holmes, E.; Woods, T.; Molloy, C.B.; Molloy, M.G.; Shanahan, F.; Cotter, P.D.; et al. The Effects of Sustained Fitness Improvement on the Gut Microbiome: A Longitudinal, Repeated Measures Case-study Approach. *Transl Sports Med* **2021**, *4*, 174-192.